

This discussion paper is/has been under review for the journal Biogeosciences (BG).
Please refer to the corresponding final paper in BG if available.

The 2009–2010 step in atmospheric CO₂ inter-hemispheric difference

R. J. Francey and J. S. Frederiksen

Earth System Assessment, CSIRO Oceans and Atmosphere Flagship, Aspendale, Australia

Received: 6 August 2015 – Accepted: 19 August 2015 – Published: 11 September 2015

Correspondence to: R. J. Francey (roger.francey@csiro.au)

Published by Copernicus Publications on behalf of the European Geosciences Union.

BGD

12, 15087–15109, 2015

The 2009–2010 step in atmospheric CO₂ inter-hemispheric difference

R. J. Francey and
J. S. Frederiksen

[Title Page](#)

[Abstract](#)

[Introduction](#)

[Conclusions](#)

[References](#)

[Tables](#)

[Figures](#)

[⏪](#)

[⏩](#)

[◀](#)

[▶](#)

[Back](#)

[Close](#)

[Full Screen / Esc](#)

[Printer-friendly Version](#)

[Interactive Discussion](#)

Abstract

The annual average CO₂ difference between baseline data from Mauna Loa and the Southern Hemisphere increased by $\sim 0.8 \mu\text{mol mol}^{-1}$ (0.8 ppm) between 2009 and 2010, a step unprecedented in over 50 years of reliable data. We find no evidence for coinciding, sufficiently large and rapid, source/sink changes. A statistical anomaly is unlikely due to the highly systematic nature of the variation in observations. An explanation for the step, and the subsequent 5 year stability in this north–south difference, involves inter-hemispheric atmospheric exchange variation. The selected data describing this episode provide a critical test for studies that employ atmospheric transport models that interpret global carbon budgets and inform management of anthropogenic emissions.

1 Introduction

The 2009–2010 increase in annual mean CO₂ difference between hemispheres, ΔC_{N-S} , was noted by Francey et al. (2013) using data from Mauna Loa (mlo, 20° N, 156° W, altitude 3.4 km) and Cape Grim (cgo, 41° S, 145° E, 0.2 km) or South Pole (spo, 90° S, 2.8 km). They reported failure of a global carbon cycle inversion model to reach consistency between the ΔC measurements and reported source–sink changes.

Their data, extended here, are based on Commonwealth Scientific and Industrial Research Organisation (CSIRO, Australia) flask sampling. Comparisons in Fig. 1a highlight the largely consistent measurements from the 1990s using data from the National Oceanic and Atmospheric Administration (NOAA, Dlugokencky et al., 2014) and Scripps Institution of Oceanography (SIO, Keeling et al., 2009) networks. A comparison is also made with a linear regression through the SIO 5-decade $\Delta C_{\text{mlo-spo}}$ record. The historic SIO record shows an increase attributed to the increase in Fossil Fuel (FF) emissions (Le Quéré et al., 2014), which occur predominantly in the Northern Hemisphere (NH); annual global FF (including the Francey et al. suggested correction) are

The 2009–2010 step in atmospheric CO₂ inter-hemispheric difference

R. J. Francey and
J. S. Frederiksen

Title Page

Abstract

Introduction

Conclusions

References

Tables

Figures

◀

▶

◀

▶

Back

Close

Full Screen / Esc

Printer-friendly Version

Interactive Discussion



scaled to run parallel to the ΔC slope in order to emphasize the unusual nature of the 2009–2010 ΔC step. From this perspective the 0.8 ppm step, if the result of an anomalous flux, would equate to a 1.6 PgCyr^{-1} (NH) source. Also obvious in Fig. 1a is the unusual post-2009 ΔC stability compared to the earlier record.

5 The dC/dt in Fig. 1b show inter-annual variability on 3 to 5 year El Niño–Southern Oscillation (ENSO) timeframes, forced primarily by climate variability on the equatorial land biosphere (Rayner et al., 2008). This variability is largely suppressed in ΔC when resulting CO_2 is mixed into both hemispheres. Methods to obtain ΔC and dC/dt from monthly data are described in Appendix A.

10 The hemispheric representativeness of extra-tropical baseline data from the selected monitoring sites is supported by a study of aircraft vertical profiles at 12 global sites, identifying mlo and cgo as being the least affected by surface CO_2 exchanges in their respective hemispheres (Stephens et al., 2007). While the spo data closely track cgo data and other mid-to-high southern latitude (SH) sites in the CSIRO network (Francey et al., 2013), the situation is less clear for mlo because of NH heterogeneity and downwind proximity to Asia. A possible contributing factor at mlo may result from geographical susceptibility to rapidly increasing SE Asian pollution, “rapidly transported to the deep tropics” (Ashford et al., 2015). However in the Supplement Fig. S1 we demonstrate similarity in year-to-year changes in ΔC using both Pacific and Atlantic
15 extra-tropical NH sites from the NOAA network. The similarity is particularly significant in sign and magnitude for the two largest observed changes in 2009–2010 and 2002–2003, implying that especially for these periods mlo represents NH behaviour.

2 Isotopic evidence for the systematic nature of ΔC variation

25 If variations in ΔC involve CO_2 of terrestrial biosphere origin (which includes FF) then a strong relationship between the changes in CO_2 concentration and changes in its stable isotope ratio $\delta^{13}\text{C}$ is expected. The $\delta^{13}\text{C}$ in CO_2 are a “reduced ratio” of $^{13}\text{C}/^{12}\text{C}$,

BGD

12, 15087–15109, 2015

The 2009–2010 step in atmospheric CO_2 inter-hemispheric difference

R. J. Francey and
J. S. Frederiksen

Title Page

Abstract

Introduction

Conclusions

References

Tables

Figures

◀

▶

◀

▶

Back

Close

Full Screen / Esc

Printer-friendly Version

Interactive Discussion

for sample s and reference r :

$$\delta^{13}\text{C}_s = \left(\frac{{}^{13}\text{C}_s/{}^{12}\text{C}_s - {}^{13}\text{C}_r/{}^{12}\text{C}_r}{{}^{13}\text{C}_r/{}^{12}\text{C}_r} \right)$$

Mass conservation in ^{13}C is approximated using the product of C and $\delta^{13}\text{C}$, i.e. $\delta^{13}\text{C}$ is approximately inversely proportional to C (Enting et al., 1995).

The CSIRO data in Fig. 2 reinforce the systematic nature of the ΔC variations with a tight linear relationship between IH differences in the CO_2 stable carbon isotope ratio and in the inverse CO_2 concentration, $(\Delta C)^{-1}$, including both the step and pre-2010 year-to-year variations ($r^2 = 0.95$). However inconsistency between laboratories, shown in Table 1, is substantial. Concentration data, particularly from CSIRO and NOAA (Masarie et al., 2001; Francey et al., 2015), are in sufficiently close agreement that the differences must lie with isotopic measurement (Appendix B). The random nature of the scatter in Fig. 2 is emphasised by a lack of correlation between NOAA and SIO $\Delta\delta^{13}\text{C}$ linear regression residuals ($r^2 \sim 0.1$).

We interpret the strong relationship using CSIRO isotope data as implying CO_2 dominated by a C3 photosynthetic signature (Farquhar et al., 1982), including FF, but excluding significant contributions from oceans or equatorial C4 plants; also implied is that the CO_2 has had little opportunity for isotopic equilibration with natural reservoirs, i.e. < 1 – 2 years since release (Enting et al., 1995).

3 Reported source/sink anomalies

If ΔC variations in Fig. 1 are indeed systematic, then clues to the forcing should be clarified by close examination of ΔC and dC/dt at the times of a number of anomalous surface flux events that have been reported over the period.

The largest such events since the 1960s that influence CO_2 are the 1991 Pinatubo volcanic eruption triggering increased removal of CO_2 from the atmosphere in subsequent years (Frölicher et al., 2013) and 1997–1998 Indonesian peat fires (Page

The 2009–2010 step in atmospheric CO_2 inter-hemispheric difference

R. J. Francey and
J. S. Frederiksen

Title Page

Abstract

Introduction

Conclusions

References

Tables

Figures

◀

▶

◀

▶

Back

Close

Full Screen / Esc

Printer-friendly Version

Interactive Discussion



et al., 2009). Taking into account that the differences between NOAA and CSIRO mlo dC/dt records are smaller after 2000 (reflecting general improvements in measurement, Francey et al., 2015) the hemispheric differences during these two events are generally small, as expected if their influences are distributed into both hemispheres.

The major non-equatorial, terrestrial emission events reported over the last 2 decades are the 2002–2003 boreal wildfires (Giglio et al., 2013), the 2008 Global Financial Crisis (Peters et al., 2012) and 2011 SH savannah growth (Poulter et al., 2014):

- the 2002–2003 event corresponds to significant N–S differences in CO₂ growth rate, dC/dt, in Fig. 1b. Year 2003 corresponds to drought in Europe “unprecedented during the last century”, releasing ~ 0.5 PgC yr⁻¹ (Ciais et al., 2005), adding to 2003 GFED4 fire emissions in boreal America and boreal Asia of 0.3 PgC, ~ 2 times the 1997–2013 mean (Giglio et al., 2013). However for emissions spread evenly over a full year, a relatively small ΔC impact is expected since the 2003 NH FF combustion was ~ 7.5 PgC compared to < 0.6 PgC from NH non-FF sources. Never-the-less 2002–2003 is, along with 2009–2010, a consistent ΔC feature using the NOAA network data (Fig. S1). A possible IH exchange contribution is explored below.

- The Global Financial Crisis (GFC) of 2007–2008 coincides in Fig. 1b with the only occasion when the NH dC/dt ENSO peak is markedly smaller than that in the SH. While 2008, 2009 are the two lowest global fire emission years in the GFED4 database, combined boreal emissions are near average, favouring the GFC as a more likely explanation for the dC/dt behaviour. However, it is less clear that relatively low 2008, 2009 ΔC in Fig. 1a are attributable to the GFC, and a possible contribution from IH exchange is also examined below.

- The 2011 event was erroneously linked to “2010–2011” ΔC changes by Poulter et al., changes which in fact occurred between 2009 and 2010 (there are no obvious changes in ΔC between 2010 and 2011, and mlo, cgo dC/dt agree in 2011). During 2009–2010, dC/dt show a larger NH ENSO peak, leading that in the SH

The 2009–2010 step in atmospheric CO₂ inter-hemispheric difference

R. J. Francey and
J. S. Frederiksen

Title Page

Abstract

Introduction

Conclusions

References

Tables

Figures

◀

▶

◀

▶

Back

Close

Full Screen / Esc

Printer-friendly Version

Interactive Discussion



by around 6 months, a phase difference not observed for other significant El Niño peaks in Fig. 1b. This implies either an undetected NH source or changes in IH transport.

Independent evidence for the NH origin of the 2009 to 2010 CO₂ ΔC step comes from a recent analysis of upper troposphere measurements for 11 latitude bands between 30° N to 30° S (Matsueda et al., 2015) where the step is evident north of 10° N. These authors suggest a role for transport, as well as source/sinks, to explain their year-to-year variations in latitudinal differences.

4 Anomalies in annual interhemispheric mixing

Meridional transport and eddy mixing due to large scale eddy motions are sources of significant uncertainty in estimations of IH transport (Miyazaki et al., 2008). Here we examine the role of the opening and closing of the upper tropospheric equatorial westerly duct, and associated inter-hemispheric Rossby wave propagation, as a contributor to the 2009–2010 ΔC_{mlo-cgo} shift, and other variations, shown in Fig. 1a.

Extra-tropical NH Rossby waves, including a branch of the Himalayan wave-train, are able to penetrate into the SH when near-equatorial zonal winds are westerly in the upper tropospheric duct centred on 140 to 170° W and 5° N to 5° S (Webster and Holton, 1982; Frederiksen and Webster, 1988; Webster and Chang, 1988). This region is delineated and its tropospheric relevance revealed in Fig. 3a showing strongly correlated upper tropospheric westerly winds with the Southern Oscillation Index (SOI) over the full 1949 to 2011 wind reanalysis dataset (<http://www.esrl.noaa.gov/psd/data/gridded/data.ncep.reanalysis.html>).

The wind direction and strength (u_{duct}) in this duct are determined by seasonal and ENSO sea-surface temperature variations; the upper troposphere westerlies are strongest in the boreal winter, and during La Nina periods, when they are correlated with proportional increases in near-equatorial transient kinetic energy (Fig. 6, Frederiksen and Webster, 1988) which facilitates inter-hemispheric mixing of trace gases. At

The 2009–2010 step in atmospheric CO₂ inter-hemispheric difference

R. J. Francey and
J. S. Frederiksen

Title Page

Abstract

Introduction

Conclusions

References

Tables

Figures

◀

▶

◀

▶

Back

Close

Full Screen / Esc

Printer-friendly Version

Interactive Discussion



other times, including El Niños, the u_{duct} are near zero or easterly, causing the Rossby wave eddies to be deflected northwards and dissipated in the equatorial regions, inhibiting inter-hemispheric exchange.

For the period July 2009 to June 2010 the average 300 hPa equatorial zonal winds in the duct region were easterly as shown in Fig. 3c, effectively closing the duct and increasing the build-up of FF CO₂ in the NH. The July 2008 to June 2009 open duct pattern, with westerlies in the duct, is shown in Fig. 3d. (Appendix C addresses the altitude range involved in this process. Note also, the meridional wind may make a small contribution to IH transport in the duct region during this time).

Figure 3b shows the 300 hPa zonal winds for July 2008 to June 2009 (Fig. 3d) minus those for July 2009 to June 2010 (Fig. 3c) and the pattern bears strong similarities with the long-term zonal wind vs. SOI correlation in Fig. 3a.

5 Trace gas interhemispheric exchange through the duct

Inter-hemispheric exchange of a seasonally varying gas by this process depends on co-variance with u_{duct} , and is represented in Fig. 4 by the product of monthly u_{duct} and ΔC for routinely monitored CSIRO species C= CO₂, CH₄, CO and H₂. The direction of a step in ΔC depends on the magnitude and sense of the trace gas IH gradient when the duct is open. The seasonality at mlo and cgo for the different gases are given in Fig. S2.

In the top panel monthly u_{duct} are plotted over red and blue shading representing El Niño and La Niña periods respectively. We add symbols connected by a solid line that are an integration of the NH winter peaks, Σu_{duct} (October to April) for a nominal $u_{\text{duct}} > 2 \text{ ms}^{-1}$, in order to better compare year-to-year changes in the strength and duration of the seasonal duct exchange.

Over the NH winters starting in 1995, 1997 and 2010 when Σu_{duct} is $< 10 \text{ ms}^{-1}$, the ΔC in Fig. 1a shows the three largest step increases. (Note: the strength of the 1997/98 event is possibly complicated by record tropical wild-fire emissions estimated

BGD

12, 15087–15109, 2015

The 2009–2010 step in atmospheric CO₂ inter-hemispheric difference

R. J. Francey and
J. S. Frederiksen

Title Page

Abstract

Introduction

Conclusions

References

Tables

Figures

◀

▶

◀

▶

Back

Close

Full Screen / Esc

Printer-friendly Version

Interactive Discussion



to missing data (particularly at spo) and measurement bias (Francey et al., 2015) and not considered further here. The 1986–1988 event most mirrors 2009–2010 being the next largest step, followed by four years of relatively stable ΔC .

We conclude from this that anomalies in the inter-hemispheric exchange through the duct have played a significant ongoing role in modifying spatial differences in CO_2 (and other trace species) at the surface. As NH FF CO_2 emissions increase further, the influence is expected to become more marked in $\Delta C \times u_{duct}$.

7 Conclusions

Peylin et al. (2013) describe conflict between groups of models in locating the major global terrestrial sink, whether mid-northern latitude or equatorial, and suggest atmospheric transport implementations may be involved. We have presented a variety of complementary evidence linking interhemispheric transport through the Pacific upper troposphere equatorial duct and the spatial and temporal difference in measured surface CO_2 concentrations. The observed patterns of CO_2 inter-hemispheric changes are not easily explained by observed source/sink behaviour.

The observed 2009–2010 changes in CO_2 IH difference in particular, because of the magnitude and absence of plausible reported source/sink changes (in a time of unprecedented monitoring of ecosystem and ocean exchanges), provide an unusual opportunity to test the implementation of atmospheric transport in inversion models and help remove current ambiguities between surface exchanges and transport. More generally, this requires such models to demonstrate an ability to describe the spatial and temporal systematic differences in selected high-quality baseline trace gas records that have well established large-scale representation, such as the mlo-cgo records used here.

The 2009–2010 step in atmospheric CO_2 inter-hemispheric difference

R. J. Francey and
J. S. Frederiksen

Title Page

Abstract

Introduction

Conclusions

References

Tables

Figures

◀

▶

◀

▶

Back

Close

Full Screen / Esc

Printer-friendly Version

Interactive Discussion

Appendix A: Trace gas data processing

The analyses for both dC/dt and ΔC are based on monthly average mixing ratios (or $\delta^{13}C$ isotopic ratios) obtained from a smooth curve through individual flask data (typically 4 month^{-1}) with combined harmonic (seasonal) and 80 day smoothing spline (Thoning et al., 1989). At Cape Grim, selected data represent strong near-surface winds ($> 5 \text{ ms}^{-1}$, 164 m.a.s.l.) with trajectories (typically > 10 days) over the Southern Ocean; at Mauna Loa samples are collected in moderate down-slope winds; South Pole samples are selected to avoid local (station) contamination. Conventional smoothing splines through de-seasonalised baseline-selected concentration data, with 50 % attenuation at 22 months, are differentiated to provide dC/dt since 1992; Francey et al. (2015) discuss dC/dt uncertainties. Annually averaged ~ 80 day smoothed monthly baseline concentration data are used to provide ΔC with near-annual time resolution, i.e. potential ambiguity between seasonality and inter-annual variation is addressed differently by dC/dt and ΔC . CSIRO and NOAA data are processed identically. Scripps data used here are monthly data that are seasonally adjusted and filled (<http://scrippsco2.ucsd.edu>).

(Note: Using the spatial differences from individual laboratories effectively removes most calibration issues that can complicate high precision comparisons of data between laboratories.) CO_2 differences between NOAA and CSIRO same-air comparisons since 1992 are $0.11 \pm 0.13 \text{ ppm}$, with mean difference effectively cancelled in mlo-cgo comparisons. This means the maximum $\delta^{13}C$ measurement error due to CO_2 difference should be less than 0.005 ‰ .

Appendix B: Laboratory differences in $\delta^{13}C$ data

A linear regression between $\Delta\delta^{13}C$ and ΔC for the pre-2010 CSIRO mlo-cgo data gives: $\Delta\delta^{13}C = 0.050(\pm 0.004) \times \Delta C + 0.062$, $r^2 = 0.92$ with slope $0.05 \text{ ‰} \times \text{ppm}^{-1}$ characteristic of exchange with terrestrial C3 plants, including FF (which are fractionated

BGD

12, 15087–15109, 2015

The 2009–2010 step in atmospheric CO_2 inter-hemispheric difference

R. J. Francey and
J. S. Frederiksen

Title Page

Abstract

Introduction

Conclusions

References

Tables

Figures

◀

▶

◀

▶

Back

Close

Full Screen / Esc

Printer-friendly Version

Interactive Discussion



(July 2008 to June 2009) minus (July 2009 to June 2010) zonal wind difference (Fig. 3b) is largely equivalent barotropic with similar strength between 300 and 100 hPa and reducing at the upper and lower levels. Northern winter (DJF) differences for 2008/09 minus 2009/10 are circa twice as strong in the westerly duct region as those in Fig. 3b.

5 **The Supplement related to this article is available online at doi:10.5194/bgd-12-15087-2015-supplement.**

Author contributions. R. J. Francey provided trace gas information and J. S. Frederiksen the atmospheric dynamics information.

10 *Acknowledgements.* This paper relies on the decades-long commitment by skilled CSIRO GASLAB scientific personnel, particularly Paul Steele, Ray Langenfelds, Paul Krummel, Colin Allison, Paul Fraser and Marcel van der Schoot; many support staff in GASLAB, Cape Grim Baseline Air Pollution Station (The Australian Bureau of Meteorology with CSIRO), and measurement collaborators at NOAA, also contribute directly in this regard. The importance of the historic SIO records cannot be understated. Rachel Law provided global, and Ying Ping Wang with Chris Lu regional, CO₂ modelling advice.

References

- 15 Ashfold, M. J., Pyle, J. A., Robinson, A. D., Meneguz, E., Nadzir, M. S. M., Phang, S. M., Samah, A. A., Ong, S., Ung, H. E., Peng, L. K., Yong, S. E., and Harris, N. R. P.: Rapid transport of East Asian pollution to the deep tropics, *Atmos. Chem. Phys.*, 15, 3565–3573, doi:10.5194/acp-15-3565-2015, 2015.
- 20 Ciais, Ph., Reichstein, M., Viovy, N., Granier, A., Ogée, J., Allard, V., Aubinet, M., Buchmann, N., Bernhofer, Chr., Carrara, A., Chevallier, F., De Noblet, N., Friend, A. D., Friedlingstein, P., Grünwald, T., Heinesch, B., Keronen, P., Knohl, A., Krinner, G., Loustau, D., Manca, G., Matteucci, G., Miglietta, F., Ourcival, J. M., Papale, D., Pilegaard, K., Rambal, S., Seufert, G., Soussana, J. F., Sanz, M. J., Schulze, E. D., Vesala, T., and Valentini, R.: Europe-wide reduction in primary productivity caused by the heat and drought in 2003, *Nature*, 437, 529–533, doi:10.1038/nature03972, 2005.

The 2009–2010 step in atmospheric CO₂ inter-hemispheric difference

R. J. Francey and
J. S. Frederiksen

Title Page

Abstract

Introduction

Conclusions

References

Tables

Figures

◀

▶

◀

▶

Back

Close

Full Screen / Esc

Printer-friendly Version

Interactive Discussion



BGD

12, 15087–15109, 2015

**The 2009–2010 step
in atmospheric CO₂
inter-hemispheric
difference**R. J. Francey and
J. S. Frederiksen[Title Page](#)[Abstract](#)[Introduction](#)[Conclusions](#)[References](#)[Tables](#)[Figures](#)[◀](#)[▶](#)[◀](#)[▶](#)[Back](#)[Close](#)[Full Screen / Esc](#)[Printer-friendly Version](#)[Interactive Discussion](#)

Jain, A. K., Johannessen, T., Kato, E., Keeling, R. F., Kitidis, V., Klein Goldewijk, K., Koven, C., Landa, C. S., Landschützer, P., Lenton, A., Lima, I. D., Marland, G., Mathis, J. T., Metz, N., Nojiri, Y., Olsen, A., Ono, T., Peng, S., Peters, W., Pfeil, B., Poulter, B., Raupach, M. R., Regnier, P., Rödenbeck, C., Saito, S., Salisbury, J. E., Schuster, U., Schwinger, J., Séférian, R., Segschneider, J., Steinhoff, T., Stocker, B. D., Sutton, A. J., Takahashi, T., Tilbrook, B., van der Werf, G. R., Viovy, N., Wang, Y.-P., Wanninkhof, R., Wiltshire, A., and Zeng, N.: Global carbon budget 2014, *Earth Syst. Sci. Data*, 7, 47–85, doi:10.5194/essd-7-47-2015, 2015.

Locatelli, R., Bousquet, P., Chevallier, F., Fortems-Cheney, A., Szopa, S., Saunois, M., Agustí-Panareda, A., Bergmann, D., Bian, H., Cameron-Smith, P., Chipperfield, M. P., Gloor, E., Houweling, S., Kawa, S. R., Krol, M., Patra, P. K., Prinn, R. G., Rigby, M., Saito, R., and Wilson, C.: Impact of transport model errors on the global and regional methane emissions estimated by inverse modelling, *Atmos. Chem. Phys.*, 13, 9917–9937, doi:10.5194/acp-13-9917-2013, 2013.

Masarie, K. A., Langenfelds, R. L., Allison, C. E., Conway, T. J., Dlugokencky, E. J., Francey, R. J., Novelli, P. C., Steele, L. P., Tans, P. P., Vaughn, B., and White, J. W. C.: NOAA/CSIRO Flask Air Intercomparison Experiment: a strategy for directly assessing consistency among atmospheric measurements made by independent laboratories. *J. Geophys. Res.*, 106, 20445–20464, 2001.

Matsueda, H., Machida, T., Sawa, Y., and Niwa, Y.: Long-term change of CO₂ latitudinal distribution in the upper troposphere, *Geophys. Res. Lett.*, 42, 2508–2514, doi:10.1002/2014GL062768, 2015.

Miyazaki, K., Patra, P. K., Takigawa, M., Iwasaki, T., and Nakazawa, T.: Global-scale transport of carbon dioxide in the troposphere, *J. Geophys. Res.*, 113, D15, doi:10.1029/2007JD009557, 2008.

Page, S. E., Hoscilo, Langner, A., A., Tansey, K. J., Siegert, F., Limin, S. H., and Rieley, J. O.: Tropical peatland fires in Southeast Asia, in: *Tropical Fire Ecology: Climate Change, Land Use and Ecosystem Dynamics*, edited by: Cochrane, M. A., Springer-Praxis, Heidelberg, Germany, 263–287, 2009.

Poulter, B., Frank, D., Ciais, P., Myneni, R. B., Andela, N., Bi, J., Broquet, G., Canadell, J. G., Chevallier, F., Liu, Yi, Y., Running, S. W., Sitch, S., and van der Werf, G. R.: Contribution of semi arid ecosystems to inter-annual variability of the global carbon cycle, *Nature*, 509, 600–603, doi:10.1038/nature13376, 2014.

BGD

12, 15087–15109, 2015

**The 2009–2010 step
in atmospheric CO₂
inter-hemispheric
difference**R. J. Francey and
J. S. Frederiksen[Title Page](#)[Abstract](#)[Introduction](#)[Conclusions](#)[References](#)[Tables](#)[Figures](#)[◀](#)[▶](#)[◀](#)[▶](#)[Back](#)[Close](#)[Full Screen / Esc](#)[Printer-friendly Version](#)[Interactive Discussion](#)

- Rayner, P. J., Law, R. M., Allison, C. E., Francey, R. J., Trudinger, C. M., and Pickett-Heaps, C.: Interannual variability of the global carbon cycle (1992–2005) inferred by inversion of atmospheric CO₂ and $\delta^{13}\text{CO}_2$ measurements, *Global Biogeochem. Cy.*, 22, GB3008, doi:10.1029/2007GB003068, 2008.
- 5 Stephens, B. B., Gurney, K. R., Tans, P. P., Sweeney, C., Peters, W., Bruhwiler, L., Ciais, P., Ramonet, M. I. Bousquet, P., Nakazawa, T., Aoki, S., Machida, T., Inoue, G., Vinnichenko, N., Lloyd, J. Jordan, A., Heimann, M., Shibistova, O., Langenfelds, R. L., Steele, L. P., Francey, R. J., and Denning, A. S., Weak Northern and Strong Tropical Land Carbon Uptake from Vertical Profiles of Atmospheric CO₂, *Science*, 316, 1732–1735, 2007.
- 10 Thoning, K. W., Tans, P. P., and Komhyr, W. D.: Atmospheric carbon dioxide at Mauna Loa observatory, 2, Analysis of the NOAA/GMCC data, 1974–1985, *J. Geophys. Res.*, 94, 8549–8565, 1989.
- Webster, P. J. and Chang, H.-R.: Equatorial energy accumulation and emanation regions: impacts of a zonally varying basic state, *J. Atmos. Sci.*, 45, 803–829, 1988.
- 15 Webster, P. J. and Holton, J. R.: Cross-equatorial response to mid-latitude forcing in a zonally varying basic state, *J. Atmos. Sci.*, 39, 722–733, 1982.

The 2009–2010 step in atmospheric CO₂ inter-hemispheric difference

R. J. Francey and
J. S. Frederiksen

Title Page

Abstract

Introduction

Conclusions

References

Tables

Figures

◀

▶

◀

▶

Back

Close

Full Screen / Esc

Printer-friendly Version

Interactive Discussion

Table 1. Coefficients in linear regressions between the annual mean CO₂ stable isotope difference and the inverse of the annual mean CO₂ concentration difference between mlo and either cgo (CSIRO, NOAA) or spo (SIO).

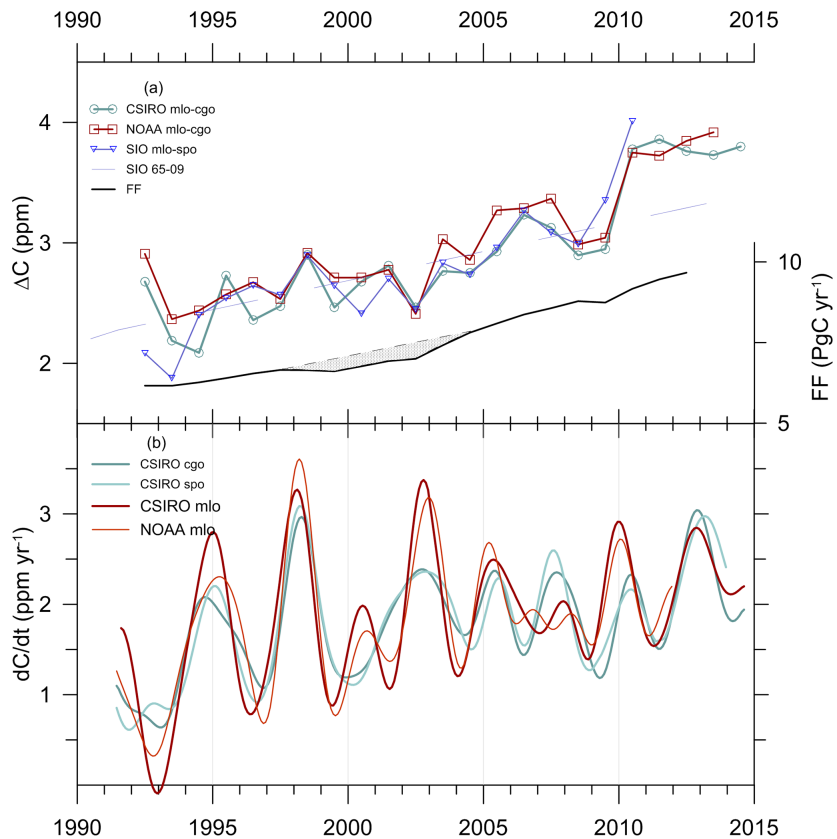
$\Delta\delta^{13}\text{C} = a \times (\Delta\text{C})^{-1} + b$	a	b	r^2
CSIRO	0.35	-0.20	0.95
NOAA	0.33	-0.19	0.56
SIO	0.15	-0.12	0.32

BGD

12, 15087–15109, 2015

The 2009–2010 step in atmospheric CO₂ inter-hemispheric difference

R. J. Francey and
J. S. Frederiksen



15103

[Title Page](#)
[Abstract](#)
[Introduction](#)
[Conclusions](#)
[References](#)
[Tables](#)
[Figures](#)
[◀](#)
[▶](#)
[◀](#)
[▶](#)
[Back](#)
[Close](#)
[Full Screen / Esc](#)
[Printer-friendly Version](#)
[Interactive Discussion](#)


Figure 1. North–South differences and growth rates in CO₂ since 1990: **(a)** on the left axis, annual average (January–December) ΔC (ppm) from three programs, CSIRO, NOAA (mlo-cgo) and SIO (mlo-spo), plotted mid-year. On the right axis are reported anthropogenic emissions (dashed line), with the Francey et al. (2013) suggested correction (shaded), scaled so that the overall slope is similar to that from the long term mlo-spo SIO record. **(b)** CSIRO (mlo, cgo, spo) and NOAA (mlo) growth rates, dC/dt , plotted mid-month. See the Supplement for CSIRO data and methods.

BGD

12, 15087–15109, 2015

The 2009–2010 step in atmospheric CO₂ inter-hemispheric difference

R. J. Francey and
J. S. Frederiksen

Title Page

Abstract

Introduction

Conclusions

References

Tables

Figures

◀

▶

◀

▶

Back

Close

Full Screen / Esc

Printer-friendly Version

Interactive Discussion

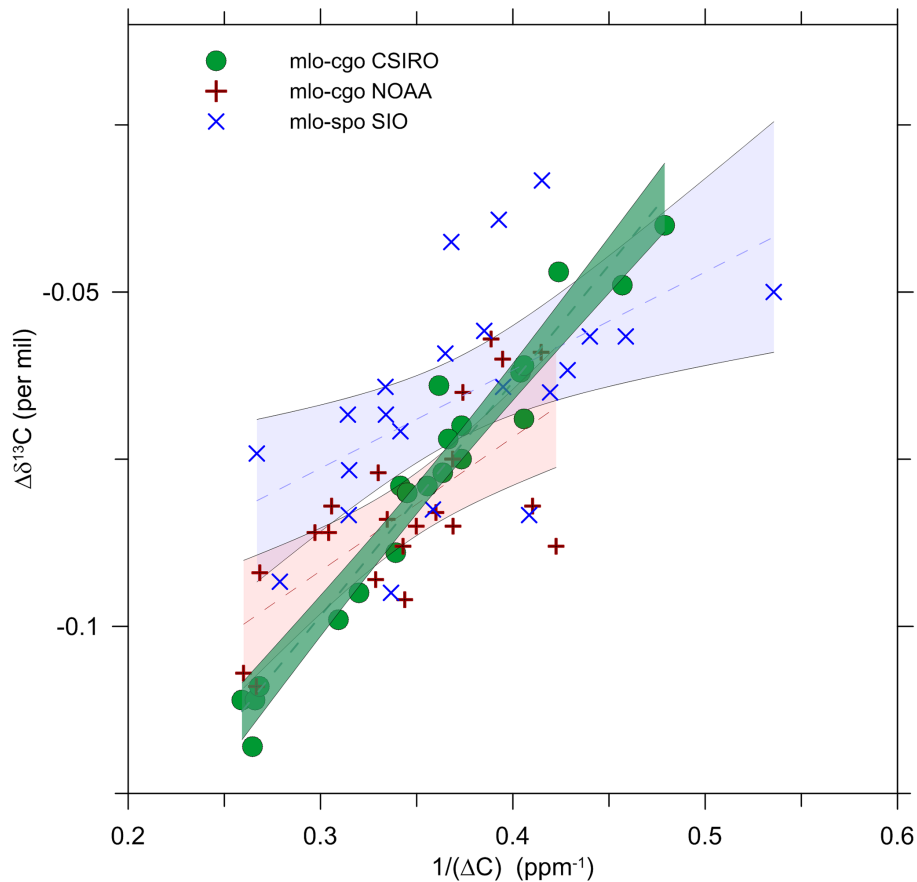


Figure 2. Isotopic evidence for systematic interhemispheric CO₂ variations: annual average North–South $\delta^{13}\text{C}$ differences vs. $(\Delta\text{C})^{-1}$, for CSIRO mlo-cgo (green), NOAA mlo-cgo (red) and SIO mlo-spo (blue). 95% confidence intervals for linear regressions are shown. One 2003 NOAA outlier ($> 5\sigma$), is removed from these plots and regressions.

The 2009–2010 step in atmospheric CO₂ inter-hemispheric difference

R. J. Francey and J. S. Frederiksen

Title Page

Abstract Introduction

Conclusions References

Tables Figures

◀ ▶

◀ ▶

Back Close

Full Screen / Esc

Printer-friendly Version

Interactive Discussion

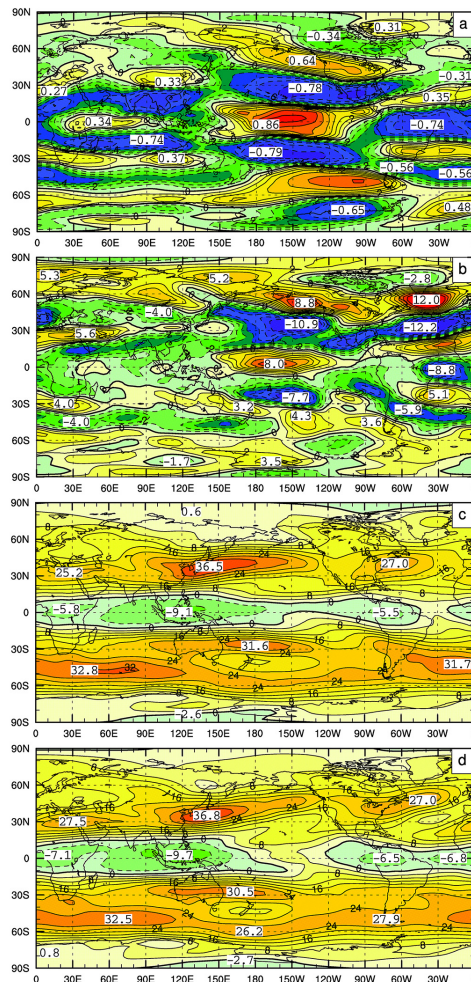


BGD

12, 15087–15109, 2015

The 2009–2010 step in atmospheric CO₂ inter-hemispheric difference

R. J. Francey and
J. S. Frederiksen



Title Page

Abstract

Introduction

Conclusions

References

Tables

Figures



Back

Close

Full Screen / Esc

Printer-friendly Version

Interactive Discussion



Figure 3. The equatorial upper troposphere duct: **(a)** correlation over the annual cycle of 1949–2011 upper tropospheric winds (300 hPa) with the Southern Oscillation Index (SOI), with strongest correlation in the equatorial Pacific duct. **(b)** The difference between open and closed equatorial duct patterns of **(c)** and **(d)**, showing similarity to the long-term correlation pattern in **(a)**. **(c)** July 2009 to June 2010 “closed-duct” pattern with 300 hPa easterly zonal wind in the equatorial duct. **(d)** July 2008 to June 2009 “open-duct” pattern with 300 hPa westerly zonal winds in the equatorial duct.

BGD

12, 15087–15109, 2015

The 2009–2010 step in atmospheric CO₂ inter-hemispheric difference

R. J. Francey and
J. S. Frederiksen

Title Page

Abstract

Introduction

Conclusions

References

Tables

Figures

◀

▶

◀

▶

Back

Close

Full Screen / Esc

Printer-friendly Version

Interactive Discussion

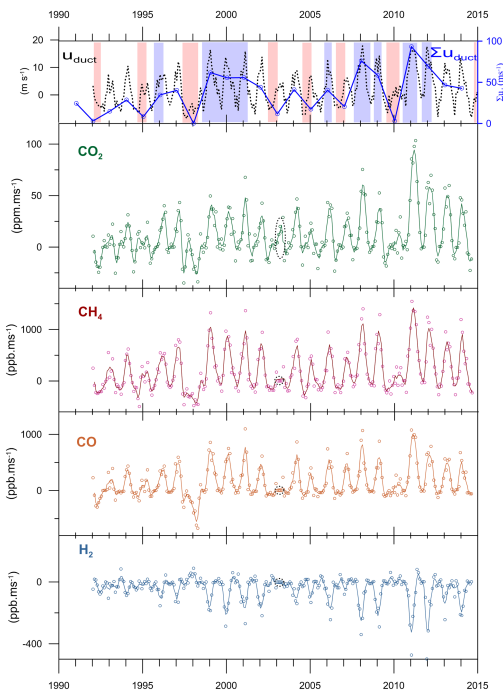


Figure 4. Monthly inter-hemispheric exchange for CSIRO trace gas species: the top panel shows monthly u_{duct} (300 hPa, 5° N to 5° S, 140 to 170° W) with red and blue bands indicating El Niño and La Niña periods respectively. The relative strength and duration of NH winter (October to April) IH mixing is estimated by Σu_{duct} , plotted in January. The following panels show the relative interhemispheric exchange fluxes ($\Delta C \times u_{duct}$), due to Pacific upper level equatorial turbulence, for different CSIRO flask species (CO_2 , CH_4 , CO and H_2). Black circles indicate 4 months of missing CSIRO flask data from mlo; for CO_2 , data from these months are obtained from NOAA records.

The 2009–2010 step in atmospheric CO_2 inter-hemispheric difference

R. J. Francey and
J. S. Frederiksen

Title Page

Abstract

Introduction

Conclusions

References

Tables

Figures

◀

▶

◀

▶

Back

Close

Full Screen / Esc

Printer-friendly Version

Interactive Discussion

The 2009–2010 step in atmospheric CO₂ inter-hemispheric difference

R. J. Francey and
J. S. Frederiksen

Title Page

Abstract

Introduction

Conclusions

References

Tables

Figures



Back

Close

Full Screen / Esc

Printer-friendly Version

Interactive Discussion

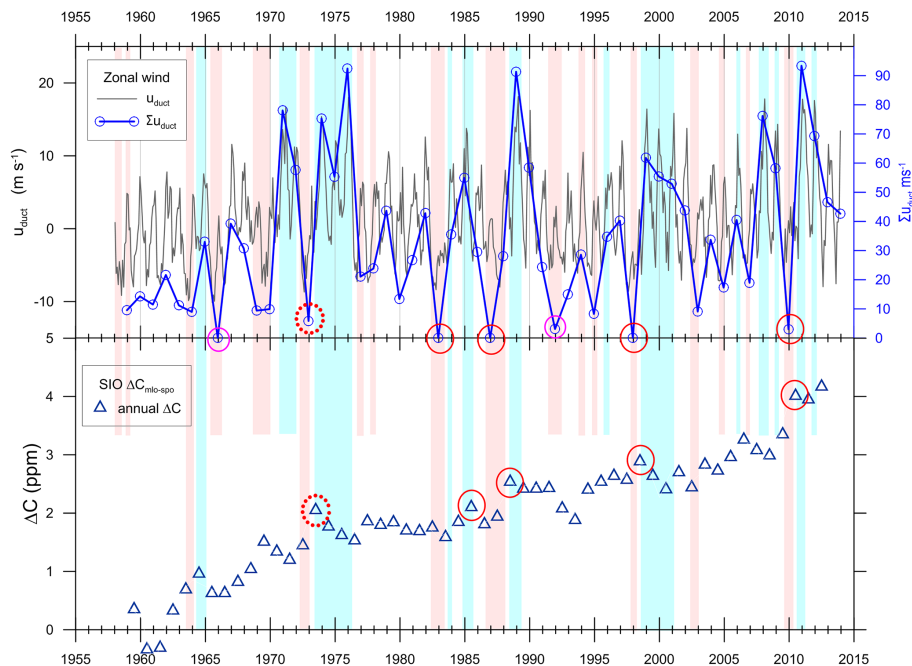


Figure 5. Inter-hemispheric mlo-spo differences from the historic Keeling record: the top panel shows monthly u_{duct} (300 hPa, 5° N to 5° S, 140 to 170° W) with red and blue bands indicating El Niño and La Niña periods respectively (left axis). The relative strength and duration of NH winter (October to April) IH mixing is estimated by Σu_{duct} , plotted in January (right axis). In the bottom panel annual average mlo-spo ΔC are shown. Red circles indicate occasions when integrated duct transport is $< 5 \text{ m}^2 \text{ s}^{-1}$, dashed for $> 5 \text{ m}^2 \text{ s}^{-1}$, and smaller circles (in the top panel) when brief closures are not followed by La Niña and there is no detectable ΔC influence.